

FE Analysis of Cyclists Kinematics and Lower Extremity Injuries in Vehicle Side Collisions

Wei HE¹, Yong HAN^{1,2}, Quan LI¹, Bingyu WANG^{1,2}

1.Xiamen University of Technology, Xiamen, China, 361024, E-mail: yonghan@xmut.edu.cn

2.Fujian Collaborative innovation center for R&D of coach and special vehicle, Xiamen, China, 361024

Abstract: Two-wheelers as a vulnerable road users are exposed to the traffic environment without protection with increased frequency and severity of accidents. The primary objective of this paper was to investigate the effect of the impact positions on the cyclist's lower extremity injury in vehicle side collisions. First, three collision cases were simulated with three different impact locations using a simulation with FE models of the human, bicycle and car. Impact kinematics of the cyclist were compared from side view and top view among the cases. In the right position, the knee of the cyclist made contact with the bonnet leading edge and shear loading was generated resulting in ruptured knee ligaments. In order to protect cyclist in collisions, it is necessary to understand what influence these impact positions have on the global kinematics and injuries of the cyclist.

Keywords: Two-wheelers, Finite element analysis, Kinematics, Lower extremity injury

1 Introduction

Traffic accidents have been becoming the important factors threatening the safety of human life, especially vulnerable road users are exposed to the traffic environment without protection with increased frequency and severity of accidents. WHO pointed out that the number of road traffic deaths each year has not increased but the number is still large (about 1.24 million per year), 50% of the world's traffic deaths occur among motorcyclists (23%), pedestrians (22%) and cyclists (5%)^[1]. In 2013, 84,589 people died from road traffic injuries, among 39% of deaths were pedestrians, cyclists and motorcyclists in the European region^[2]. Based on the police reported data in China, 21717 rider died in traffic accidents accounting for 36.2% of the annual road accident fatalities among motorcyclists (21.43%), E-bike (8.86%) and cyclists (5.91%) in 2012^[3]. Currently, more than 60 million bicycles and 120 million e-bike exist in China. With the development of bicycle-sharing, more and more people choose to use a bike during a short trip in China. The world is facing the severe challenges on the issue of the two-wheelers traffic safety with the growth of two-wheelers.

Previously, Researchers have conducted many studies of the global kinematics of cyclists during vehicle-cyclist collisions. Multi-body analysis of vehicle-cyclist collisions was introduced by Janssen et al. and is widely used to investigate the kinematics of cyclists^[4]. Peng et al. selected 22 pedestrian and 18 bicyclist accidents for reconstruction to make a comparable analysis^[5]. Ito et al. investigated the cyclist kinematics and injury risks in side collision using the Total Human Model of Safety (THUMS) FE model^[6]. Published studied indicated that head is the body region with the most frequent and sever injuries for rider. Str. et al. analyzed 114 bicyclists' accident cases and showed that 69% of fatal cyclists result from head injury^[7]. Bourdet N et al. analyzed 24 bicyclists' accident cases from both French and German accident databases, and showed that the impact against a vehicle occurs more often on the lateral top of the head base on the reconstruction of the real-world accidents^[8].

However, in vehicle collisions accident, the lower extremities of cyclists are mostly impacted directly against cars. Simms and Wood evaluated injury mechanisms and injury threshold of the lower extremities of pedestrians^[9]. Cardot et al. used a complete finite element model to simulate the car-bicycle impact, the injury analysis was quantified by stress levels on the bone structures and by strain for knee ligaments^[10]. Mizuno et al. investigated various cyclic postures of the lower extremities and showed that these postures have an important influence on the global kinematics and injuries of the cyclists^[11]. Neal-Sturgess et al. analyzed the in-depth accident data and showed that knee injuries resulting from being

impacted by the hood leading edge account for 14% of the injuries in vehicle-cyclist collisions [12]. In order to protect cyclist in collisions, it is necessary to understand what influence these impact positions have on the global kinematics and injuries of the cyclist.

2 Methods

2.1 FE Model

Fig.1 shows that a FE model of a small sedan was used for simulating car-to-bicycle collisions. The car has a bumper energy absorber and a lower energy absorber which were designed to protect pedestrian lower extremities. This car model was validated based on the pedestrian headform test at 35 km/h and the legform impact test at 40 km/h^[6]. Fig.2 shows that a FE model of a bicycle (Mobike) was developed by measuring dimensions. The mass of the bicycle model was 25 kg. The bicycle FE model included approximately 75,903 elements and 83,737 nodes with an element length of 6 mm. The rotation of the pedals, handlebar, and wheels was reproduced using revolute joints about their respective axes. The bicycle uses single front forks to connect the front tire and the tires of the bicycle were constructed by the solid element. The left and right crank arms with pedals were connected and rotated about the axis of the bottom bracket.

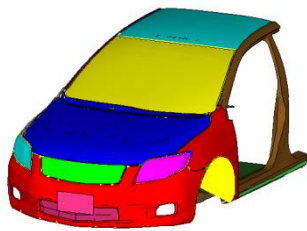


Fig. 1. Car model

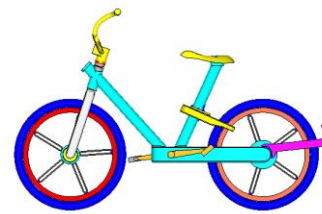


Fig. 2. Bicycle model

2.2 Simulation of Car-to-Bicycle Collision Cases

In this research study, the THUMS Version 4 AM50 Occupant Model was used as the cyclist model. The THUMS models were jointly developed by Toyota Central R&D Labs, Inc. And Toyota Motor Corporation. The human model was set to be in the posture with the right leg forward and the left backward and was placed on the bicycle model. Both left and right arms were positioned on the handlebar. The posture of the human model was changed by forced displacement applied to nodes of bones of the upper and lower extremities.

According to the analysis of two-wheelers kinematics based on the two-wheelers accident videos, approximately 70% of cases occurred at a car speed of 11.1m/s (40km/h) and approximately 60% of cases represented a collision case where the car hit the side of the two-wheelers [13]. In this simulation, the car impacted the stationary cyclist at 40 km/h. The model represented a collision case where the car hit the bicycle on the right side and selected three impact positions. Table I shows the simulation parameters and three cases were conducted. Fig.3 shows the impact positions, the first impact position (Case 2) was described as the midpoint of the front and rear wheel center of the bicycle against the centerline of the car. In other two cases (Cases 1 and 3), the midpoints were located at 600 mm left of the center of the car and right of it.

TABLE I Simulation Parameters

Case No	1	2	3
Car Speed	11.1m/s (40km/h)	11.1m/s (40km/h)	11.1m/s (40km/h)
Bicycle Speed	0	0	0
Impact Direction	Side	Side	Side
Impact Position (Centerline of car)	-600	0	600

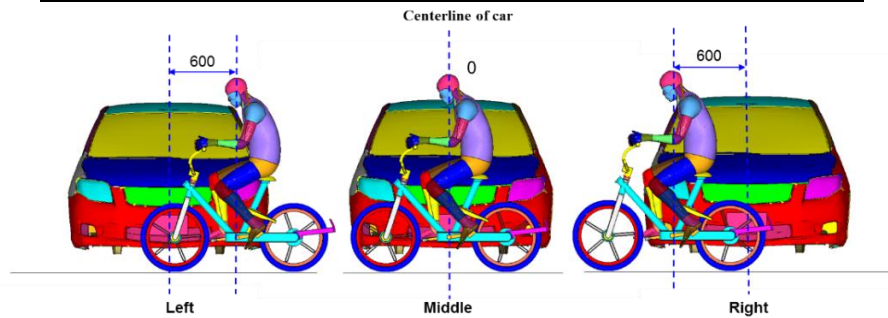


Fig. 3. Impact position (Front view)

2.3 Injury Index

In each case, the bending moment diagram of the tibia was plotted to evaluate the tibia fracture risk. The sign of the bending moment was defined as positive for the direction that the tibia deformed convex relative to the car forward direction. The fracture risk of the tibia was calculated based on the risk curve determined by Takahashi et al. [14]. The tibia bending moment was also compared to the threshold of tibia bone fracture (340 Nm) in the GTR No.9 regulation. Also, the bending angle and shear displacement of the knee were calculated to evaluate the ACL injury risk, and was compared to the threshold of ACL rupture (25.2 mm) in a pure knee shear loading condition proposed by Bose et al. [15].

3. Results

3.1 Impact Kinematics of Cyclist

Fig.4 and 5 show the side and top view of impact kinematics of the cyclists at every 40 ms in the vehicle side collisions. The head contact situation in three cases is shown in the last of the pictures. In three cases, different kinematics of cyclists were observed depending on the impact positions. In case 2, the knee and the superior part of the leg made contact with the hood leading edge. The pelvis slid over the hood top, and the bumper applied a force on the leg in the car's forward direction. Then, the femur acted as a moment-arm and the torso of the cyclist rotated about the superior-inferior axis, and the occiput of the head impacted the windshield. The global kinematics of cyclists from side view in case 1 was comparable with that of the case 2. The height of head contact point in case 1 is higher than that in case 2, because the hood length in the left position shorter than that in the middle position. However, seen from the top view, the impact of the head for the case 1 was located in the A-pillar while the case 2 in the windshield. So the head injury in case 1 is more serious than that in case 2.

In the case 3, the cyclist's kinematics was different of that in other cases. Because of the impact position, the first contact in this collision is the bicycle rather than bicyclist. The rear wheel of the bicycle firstly contacted the bumper. The foot made contact with the edge of the bumper and had a rotation. Then, the thigh contacted with the right fender and the leg had a relative sliding with the right fender. The pelvis slid over the hood top and the upper body contacted the A-pillar until the head contacted the A-pillar on the roof of the car. The thigh has a more serious injury than the leg. In comparison, the cyclist in case 3 has a large WAD compared to that in other cases, because the pelvis had a sliding with the hood top

and the head contact location is higher than that in other cases.

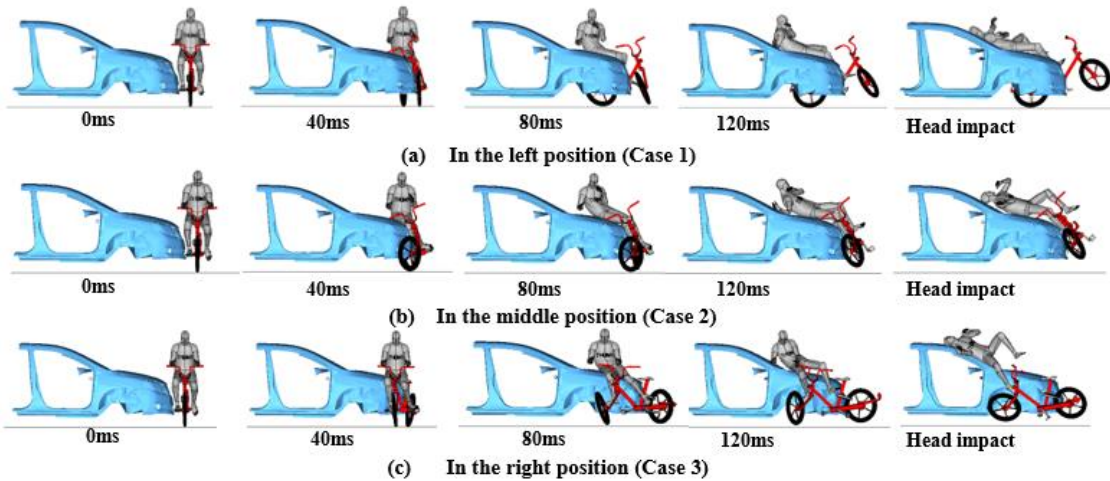


Fig. 4. Kinematics behavior of Cyclists in the vehicle side collisions(Side view)

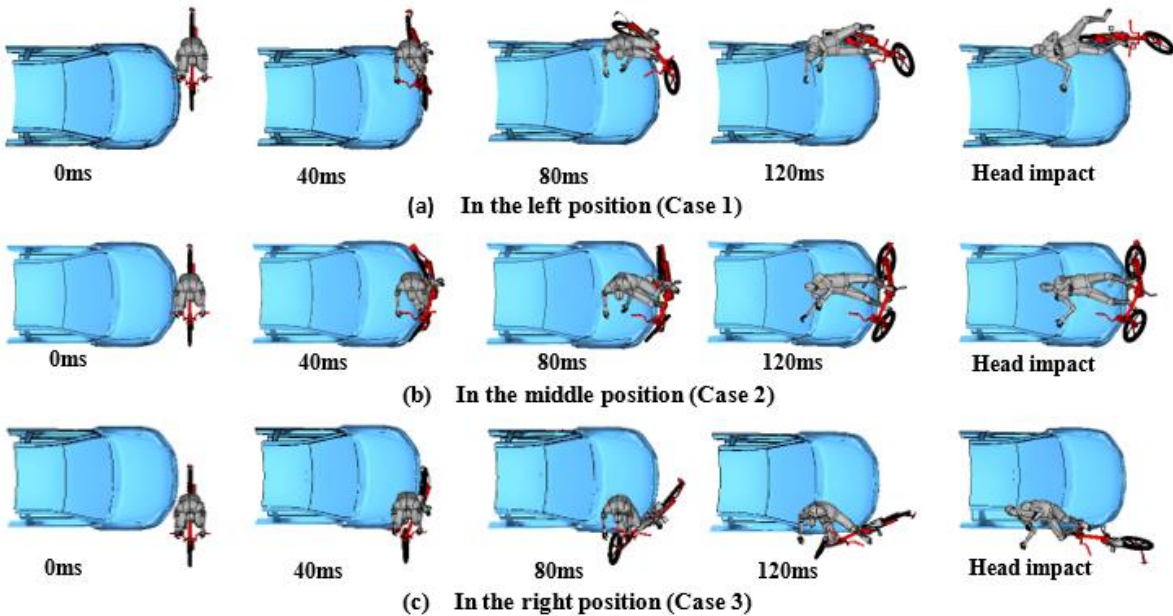


Fig. 5. Kinematics behavior of Cyclists in the vehicle side collisions(Top view)

3.2 Bending moment diagram of the tibia

Fig.6 shows the bending moment diagram of the struck tibia. As shown in Fig.6. (a) (b), the bending moment of the struck tibia in the left position is similar to that in the middle position, but their lines time is different due to the time which the tibia made contact with the hood edge is different. The proximal and distal side of the tibia contacted the hood leading edge and the bumper energy absorber, respectively. The bicycle frame impacted against the struck leg from the opposite direction. The tibia bending moment was mitigated by this opposing force from the bicycle frame. The maximum tibia bending moment was 220 Nm (3.6% fracture risk) in the left position and 123 Nm (0.3% fracture risk) in the middle position. The maximums tibia bending moment in two case were different due to the difference of impact locations characteristic of the car. The maximums were less than the threshold of tibia fracture (340 Nm).

In the right position, the bicycle firstly contacted the bumper and the struck leg made contact with the right fender. The femur of the cyclist was given a large force by the right fender and the tibia had a relative sliding with tibia, so the

right fender gave a smaller force to the tibia. The maximum tibia bending moment was 89 Nm (0.3% fracture risk) which is smaller than other two cases.

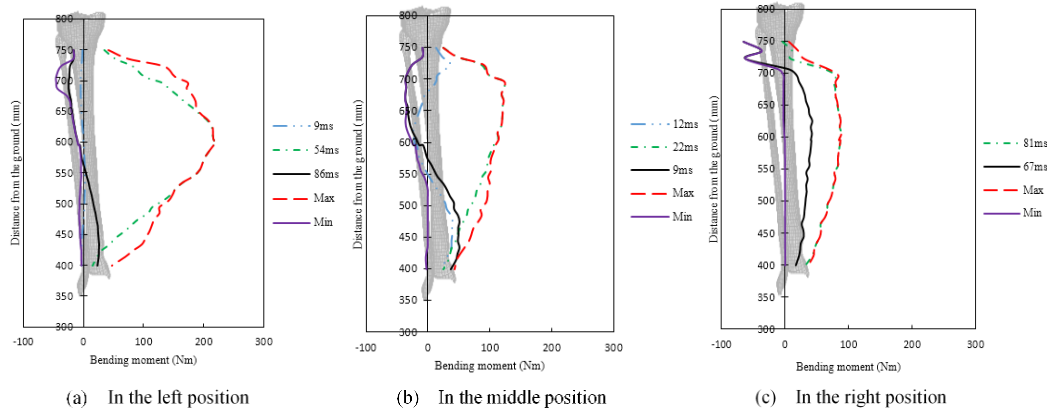


Fig. 6. Bending moment diagram of cyclists tibia

3.3 Shear displacement of the knee

The injury threshold of the bending angle of the knee is 19 degree and the knee shear displacement was compared to the threshold of ACL rupture (25.2 mm). TABLE II shows bending angle and shear displacement of the knee and their ligament injury risk in three collision cases. In the left position, the hood leading edge contacted the proximal side of the struck leg and led to a large shear loading on the knee. So the bending angle of the knee is 10.1 degree (6.2% injury risk) and shear displacement of the knee is 21.9 mm (45.2% ACL injury risk). The loading of the knee did not reach the threshold of the ACL rupture. There were no ruptures of knee ligament in this simulated condition. In the middle position, the hood leading edge contacted the proximal side of the struck leg and led to a large shear loading on the knee, which the values are similar with that in the middle position. The bending angle of the knee is 10.7 degree (6.8% injury risk) and shear displacement of the knee is 19.7 mm (33.4% ACL injury risk). There were no ruptures of knee ligament in this simulated condition.

In the right position, the values of bending angle and shear displacement are larger than those in other two cases. Though the bending moment of the tibia is small, the right fender had a large force on the femur, which has an impact on the knee. So the bending angle of the knee in the right position is 16.1 degree (20.9% injury risk) and shear displacement is 28.1 mm (79.2% ACL injury risk) which exceeded the threshold (25.2 mm). Hence, the ACL ruptured in this simulated condition.

TABLE II Bending angle and shear displacement of the knee and injury risk

Impact Position	Bending Angle (°)	Injury Risk	Shear Displacement (mm)	ACL Injury Risk
Left	10.1	6.2%	21.9	45.2%
Middle	10.7	6.8%	19.7	33.4%
Right	16.1	20.9%	28.1	79.2%

4 Conclusion

A cyclist FE model was impacted from its side by a car at 40 km/h in three different positions. In the right position, the cyclist's global kinematics is different from that in the left and middle positions, because the first contact in this collision is the bicycle rather than bicyclist. In the left position, the hood leading edge led to a relatively large tibia bending moment, though it was less than the fracture threshold. The maximums tibia bending moment in left and middle positions were different due to the difference of impact locations characteristic of the car. In the right position, the right fender gave

a small force on the struck leg and the bending moment of the tibia was small. But the cyclist's foot was impacted by the bumper and the femur was impacted by the right fender, so causing a substantial lateral shear loading of the knee, thereby resulting in an ACL rupture.

5. Acknowledgements

The authors would like to acknowledge support of the National Natural Science Foundation of China (Project No: 51775466), the Natural Science Foundation of Fujian Province, China (Project No: 2016J01748).

Reference

- [1] Global status report on road safety 2013, World Health Organization, 2015
- [2] Jackisch J, Sethi D, Mitis F, et al. 76 European facts and the global status report on road safety 2015[J]. 2015, 22(Suppl 2):A29.2-A29.
- [3] Ministry of Public Security Traffic Management Bureau, the People's Republic of China Traffic Accident Statistical Yearbook (2012), 1, Wuxi: Ministry of Public Security Traffic Management Research Institute, 2013, 58.
- [4] Janssen E G, Wismans J. EXPERIMENTAL AND MATHEMATICAL SIMULATION OF PEDESTRIAN-VEHICLE AND CYCLIST-VEHICLE ACCIDENTS[C]// INTERNATIONAL TECHNICAL CONFERENCE ON. 1985.
- [5] Peng Y, Chen Y, Yang J, et al. A study of pedestrian and bicyclist exposure to head injury in passenger car collisions based on accident data and simulations [J]. Safety Science, 2012, 50(9):1749-1759.
- [6] Ito D, Yamada H, Oida K, et al. Finite element analysis of kinematic behavior of cyclist and performance of cyclist helmet for human head injury in vehicle-to-cyclist collision[C]// 2014.
- [7] Str M M, Bj Rnstig U, N Slund K, et al. (1993). Pedal cycling fatalities in northern sweden. International Journal of Epidemiology, 22(22), 483-488.
- [8] Bourdet N, Deck C, Serre T, et al. In-depth real-world bicycle accident reconstructions [J]. International Journal of Crashworthiness, 2014, 19(3):222-232.
- [9] Simms C, Wood D. Pedestrian and Cyclist Impact [J]. Solid Mechanics & Its Applications, 2009, 166:31-49.
- [10] J Cardot, C Masson, P J Arnoux, et al. Finite element analysis of cyclist lower limb response in car [J]. International Journal of Crashworthiness, 2006, 11(2):115-130.
- [11] Mizuno K, Yamada H, Mizuguchi H, et al. The influence of lower extremity postures on kinematics and injuries of cyclists in vehicle side collisions [J]. Traffic Injury Prevention, 2016, 17(6):618-624.
- [12] Neal-Sturgess C, Carter E, Hardy R, et al. APROSYS European In-Depth Pedestrian Database [J]. Sturgess, 2007.
- [13] Yong H, Quan L, Wei H, et al. Analysis of Vulnerable Road User Kinematics Before/During/After Vehicle Collisions Based on Video Records [C]// 2017.
- [14] Konosu A, Ishikawa H. RECONSIDERATION OF INJURY CRITERIA FOR PEDESTRIAN SUBSYSTEM LEGFORM TEST -PROBLEMS OF RIGID LEGFORM IMPACTOR[C]// 2001.
- [15] Bose D, Bhalla K S, Untaroiu C D, et al. Injury tolerance and moment response of the knee joint to combined valgus bending and shear loading [J]. Journal of Biomechanical Engineering, 2008, 130(3):031008.